

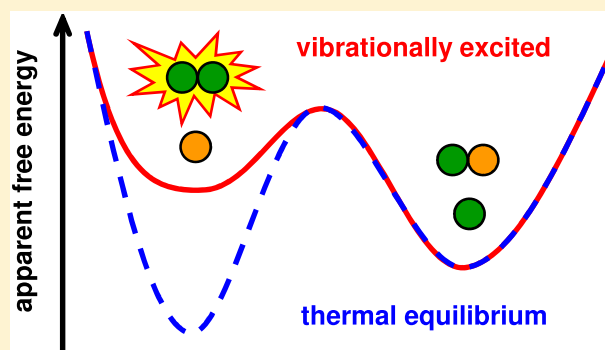
# Ensemble-Based Molecular Simulation of Chemical Reactions under Vibrational Nonequilibrium

Kristof M. Bal,<sup>\*†</sup> Annemie Bogaerts,<sup>†</sup> and Erik C. Neyts<sup>†</sup>

Research Group PLASMANT, Department of Chemistry, University of Antwerp, Universiteitsplein 1, 2610 Antwerp, Belgium

## Supporting Information

**ABSTRACT:** We present an approach to incorporate the effect of vibrational nonequilibrium in molecular dynamics (MD) simulations. A perturbed canonical ensemble, in which selected modes are excited to higher temperature while all others remain equilibrated at low temperature, is simulated by applying a specifically tailored bias potential. Our method can be readily applied to any (classical or quantum mechanical) MD setup at virtually no additional computational cost and allows the study of reactions of vibrationally excited molecules in nonequilibrium environments such as plasmas. In combination with enhanced sampling methods, the vibrational efficacy and mode selectivity of vibrationally stimulated reactions can then be quantified in terms of chemically relevant observables, such as reaction rates and apparent free energy barriers. We first validate our method for the prototypical hydrogen exchange reaction and then show how it can capture the effect of vibrational excitation on a symmetric  $S_N2$  reaction and radical addition on  $CO_2$ .



It has long been known that vibrational nonequilibrium is able to steer and control the selectivity of chemical reactions of molecules in the gas phase<sup>1–3</sup> and on surfaces.<sup>4–8</sup> Moreover, selective excitation of certain vibrational modes can be a more efficient way to thermally stimulate reactions than homogeneous heating of the whole gas.<sup>9</sup>

Plasmas are a chemical environment in which vibrational nonequilibria are naturally obtained: molecules are excited through collisions with moderately energetic ( $\sim 1$  eV) electrons.<sup>10</sup> The fact that excited vibrational states are overpopulated in many nonthermal plasmas is a key factor contributing to their unique chemical reactivity. In particular the ability of certain plasmas to carry out thermodynamically highly unfavorable processes such as  $CO_2$  dissociation with very high efficiency can be traced back to their strong nonequilibrium properties.<sup>11</sup> In addition, when interfaced with a solid catalyst,<sup>12</sup> a wealth of additional plasma-induced chemistry is obtained; here, too, stimulation of reactions by vibrational excitation has been postulated to be crucial for processes such as plasma-enabled catalytic ammonia synthesis,<sup>13</sup> methane reforming,<sup>14,15</sup> and  $CO_2$  reduction.<sup>16</sup> However, the precise mechanisms of this type of vibrationally stimulated processes and their chemical ramifications are poorly understood. Detailed atomic-level simulation approaches are therefore desirable.

Reactions of vibrationally excited molecules can be explicitly simulated with quasi-classical trajectory (QCT) methods.<sup>17</sup> However, because most chemical reactions are activated, reaction probabilities of individual collisions are quite low. This means that many trajectories (up to  $10^6$  or more for a single condition<sup>18</sup>) must be calculated in order to obtain good

statistics. QCT simulations therefore typically require a cheap potential energy surface (PES) which must be explicitly parametrized in a low-dimensional representation of the problem at hand, a restriction that has only recently been partially lifted by the advent of high-dimensional neural network potentials.<sup>19</sup>

A much more coarse-grained approach to vibrationally stimulated reactions is offered by the Fridman–Macheret (FM)  $\alpha$ -model,<sup>10</sup> in which the average rate of a reaction involving a vibrationally excited molecule is computed as a perturbation of the ground-state equilibrium rate. The FM model can be easily integrated into existing kinetic models of gas phase chemistry and thus used to assess the macroscopic impact of vibrational nonequilibrium on the overall process.<sup>20</sup> The FM model is essentially a quantitative application of Polanyi's rules of vibrational efficacy;<sup>21</sup> like Polanyi's rules, the FM model is strictly speaking applicable only to atom–diatom reactions and can hence not describe mode selectivity or gas–surface reactions, although it has been used for the latter.<sup>13</sup> The recently proposed sudden vector projection (SVP) model can explain mode selectivity as being proportional to the relative contribution of the mode to the reaction coordinate vector at the transition state.<sup>22</sup> However, just like the FM model, it does not explicitly consider the dynamics of the reactive collision and does not capture the energy dependence of reaction probabilities. Typically, the SVP method is

Received: November 13, 2019

Accepted: December 22, 2019

Published: December 23, 2019

therefore used in conjunction with QCT to rationalize the latter's findings.<sup>23</sup>

In this Letter, we introduce a new direct simulation approach within the framework of enhanced sampling techniques. On one hand, the method explicitly considers the complete dynamics of an arbitrary reacting system with excited vibrational modes. On the other hand, it can quantify the chemical effects of these excitations in terms of coarse-grained observables such as free energy barriers, reaction rate coefficients, vibrational efficiencies, and mode selectivities. This is achieved by modeling the vibrationally excited system as a perturbed canonical ensemble in which selected modes deviate from equilibrium behavior.

The main objective of our approach is to extract chemically relevant information, such as free energies and reaction rate coefficients, from simulations with atomic detail. Historically, a wide variety of free energy methods and enhanced sampling techniques has been developed specifically with the goal of providing this type of information, even for activated processes inaccessible within the time scale of unbiased MD.<sup>24</sup> However, enhanced sampling methods usually operate under the assumption of an ensemble, with macroscopic state variables such as temperature, pressure, and/or volume imposed on the system, including well-defined fluctuations and averages.

The systems we wish to simulate do not conform to a conventional ensemble. Indeed, while traditional ensembles (e.g., the canonical *NVT* ensemble) assume thermal equilibrium and a homogeneous temperature distribution, we are interested in a distinctly nonequilibrium situation. More specifically, we wish to model systems in which most modes are in equilibrium with each other at a *background temperature* ( $T_{bg}$ ), while certain selected modes have a (higher) *vibrationally excited temperature* ( $T_{vib}$ ). If the number of excited modes at  $T_{vib}$  is low, the system will generally behave as if fully equilibrated at  $T_{bg}$  with some nonequilibrium effects as a perturbation, in the spirit of the FM model. This way, reactions of molecules in thermal equilibrium can be directly compared to any of their nonequilibrium counterparts, on the same footing and using the same tools.

We approach the effect of vibrational excitation *indirectly*, in terms of probabilities. In thermal equilibrium, the probability distribution  $p(\mathbf{R})$  of any system in configuration space  $\mathbf{R}$  at temperature  $T$  and potential energy  $U(\mathbf{R})$  follows the Boltzmann distribution

$$p(\mathbf{R}) \propto e^{-\beta U(\mathbf{R})} \quad (1)$$

in which  $\beta = (k_B T)^{-1}$  and  $k_B$  is the Boltzmann constant. Similarly, the probability distribution along a reaction coordinate  $s$  can be related to the free energy surface (FES)  $F(s)$  along this coordinate, up to an irrelevant additive constant:

$$F(s) = -\frac{1}{\beta} \ln p(s) + C \quad (2)$$

Although the ensemble-based relations between energies, temperatures, and probabilities do not hold in nonequilibrium systems, the very concept of a probability distribution remains applicable. Indeed, a reaction probability can be directly correlated with the probability density at the transition state region of the reaction. Moreover, an excitation of a particular vibrational mode will result in a changed  $p(\mathbf{R})$ , which we denote as  $p^*(\mathbf{R})$ . Consequently, such a change can also be

expected to lead to a modified probability along the reaction coordinate  $p^*(s)$ , which in turn affects the reaction rate. In addition, by assuming that  $T = T_{bg}$ , a modified apparent FES  $F^*(s)$  can then be computed. These concepts are illustrated in Figure 1 for the case of a vibrationally nonadiabatic reaction.

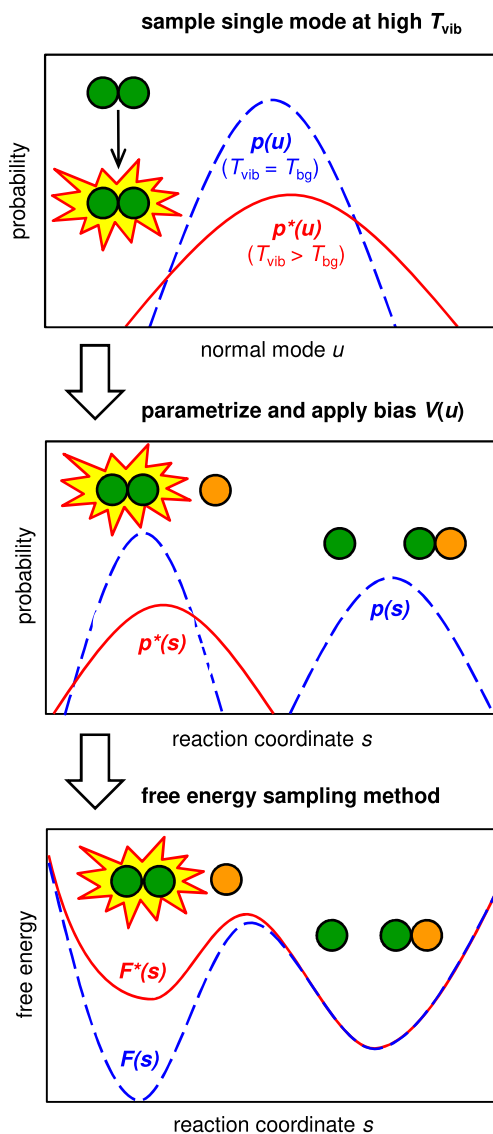


**Figure 1.** Overview of the principles behind the approach to vibrational excitation. At high  $T_{vib}$ , the probability distribution  $p^*(\mathbf{u})$  along the normal mode differs from the equilibrium distribution  $p(\mathbf{u})$  at  $T_{bg}$ . As a result, the probability distribution along a reaction coordinate  $s$  is also affected, which leads to a change in the apparent reaction free energy barrier. In our method, this modified  $F^*(s)$  (or  $p^*(s)$ ) is obtained from a free energy simulation after applying a bias potential  $V(\mathbf{u})$  that enforces  $p^*(\mathbf{u})$  at  $T_{bg}$ .

In our approach, we wish to explicitly enforce the distribution  $p^*(\mathbf{R})$  within a molecular dynamics calculation, and we use enhanced sampling methodologies to obtain  $p^*(s)$  or  $F^*(s)$ , which will allow us to characterize how specific vibrational excitation modes affect the chemistry in an arbitrary system of interest. Because of these particular choices, our method will have two key limitations that can be identified a priori.

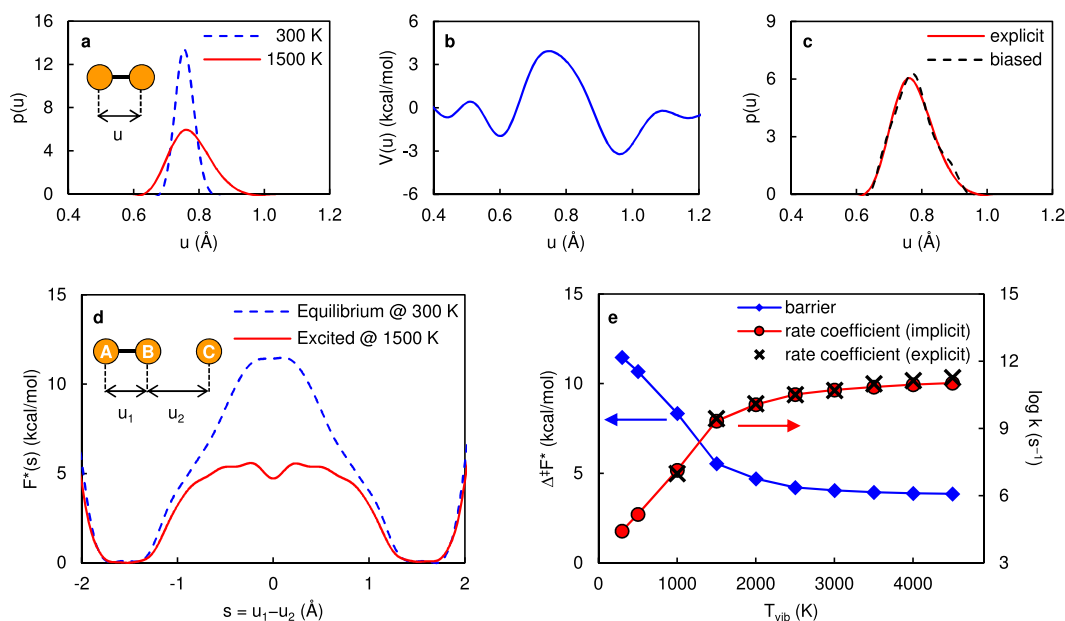


**Figure 2.** Indirect vibrational excitation method applied to the deuterium exchange reaction  $\text{D} + \text{D}_2 \rightarrow \text{D}_2 + \text{D}$ . (a) Temperature-dependent probability distribution along the D–D bond  $u$ . (b) Bias potential  $V(u)$  generating the distribution  $p^*(u)$  for  $T_{\text{vib}} = 1500$  K at  $T_{\text{bg}} = 300$  K. (c) Validation of  $V(u)$ . (d) Apparent reaction free energy surface  $F^*(s)$  at thermal equilibrium ( $T_{\text{vib}} = T_{\text{bg}} = 300$  K) and  $T_{\text{vib}} = 1500$  K obtained directly from the VES bias  $V(s)$ . Two instances of  $V(u)$  are applied to  $u_1$  and  $u_2$ , respectively, in the nonequilibrium case. (e) Apparent free energy barriers  $\Delta^\ddagger F^*$  and reaction rate coefficients  $k$  at different  $T_{\text{vib}}$ .

First, the method assumes a *purely classical energy spectrum*. As usual in MD-based canonical sampling, there is no natural way to enforce quantization of the vibrational energy. Rather, the energy stored in each mode follows a Boltzmann distribution, which is sampled over time. Such continuous distributions remain a cornerstone of our method. However, while most modes remain at  $T_{\text{bg}}$ , excited modes are at a higher  $T_{\text{vib}}$ . Physically, we therefore model the average behavior of an ensemble of excited states for modes of interest, which are Boltzmann-distributed and characterized by a temperature  $T_{\text{vib}}$ .

Second, our approach is *limited to effects in configuration space*. Although vibrational excitation has a kinetic energy component (i.e., defined in phase space), we only explicitly consider how it affects the exploration of configuration space. That is, certain reactive configurations might be sampled more (or less) in the vibrationally hot state. Our approach assumes that this change in the exploration of configuration space is what results in reaction stimulation—the actual velocities of all atoms still correspond to a (low) temperature  $T_{\text{bg}}$ . This, too, is a consequence of wanting to sample a physically defined ensemble (at least for most modes). We will however show later on that this assumption does not lead to appreciable errors.

The key advantages of our approach are that (1) it is fully atomistic without making specific mechanistic or geometric assumptions (unlike FM), (2) it is fully dynamic and explicitly considers the energies of the reacting molecules (unlike SVP), and (3) it naturally averages out the contributions of all degrees of freedom in a single simulation and can therefore run on top of a somewhat more expensive PES (unlike QCT, which requires running many independent trajectories for each specific energy or impact angle).

Our algorithm, as illustrated in Figure 1, imposes the probability distribution  $p^*(\mathbf{R})$  on a system that is otherwise conventionally thermostated at a temperature  $T_{\text{bg}}$ . Integral to

our approach is the variationally enhanced sampling (VES) method<sup>25</sup> which, beside its ability to accelerate rare events and compute free energies, is particularly useful here because it can be used to sample arbitrary “target distributions” in configuration space. This is achieved by constructing a bias potential  $V(\mathbf{u})$  as a function of a set of collective variables (CVs)  $\mathbf{u}$  through a variational optimization procedure. Given that only one particular vibrational mode is assumed to be out of equilibrium, we only have to modify the probability distribution in a small part of configuration space. Therefore, we can restrict ourselves to enforcing a distribution  $p^*(\mathbf{u})$  as a function of only a limited set of variables, while still yielding the desired distribution  $p^*(\mathbf{R})$ .

The algorithm requires three consecutive simulations. First, the target distribution  $p^*(\mathbf{u})$  must be sampled at a (high)  $T_{\text{vib}}$ , using standard histogram analysis. The choice of the CVs  $\mathbf{u}$  depends on the vibrational mode of interest (e.g., bond lengths for stretch modes, angles for bends, etc.), whereas the sampling can be carried out in a standard NVT run in the case of uncoupled vibrational modes (such as of diatomic molecules) or a “hot spot” thermostat<sup>26</sup> within the generalized Langevin equation (GLE) framework<sup>27,28</sup> in more complex cases. Second, VES is used to generate a bias potential  $V(\mathbf{u})$  that enforces the distribution  $p^*(\mathbf{u})$  within a standard NVT simulation at  $T_{\text{bg}}$ . Third, using a free energy method (in the following examples also VES, in its well-tempered variant<sup>29</sup>) and while applying the auxiliary bias  $V(\mathbf{u})$  as a fixed external potential, the apparent free energy profile  $F^*(s)$  along  $s$  can be obtained. This procedure can be repeated for any  $T_{\text{vib}}$  of interest. Of course, if  $T_{\text{vib}} = T_{\text{bg}}$ , no bias  $V(\mathbf{u})$  must be applied because  $p^*(\mathbf{u}) = p(\mathbf{u})$  (by definition).

It is important to keep in mind that many free energy methods improve sampling along  $s$  by generating an appropriate bias potential  $V(s)$ . This means that two external bias potentials will then act simultaneously on the system: the

previously optimized  $V(\mathbf{u})$  remains fixed throughout the free energy calculation, while  $V(s)$  is being generated to estimate  $F^*(s)$ .

As a first demonstration of our approach, we apply it to the prototypical H atom exchange reaction, in which hydrogen is replaced by deuterium, i.e.,  $D + D_2 \rightarrow D_2 + D$ . The only vibrational mode in this system is the D–D stretch vibration, which can be represented through the D–D bond distance as single collective variable  $u$ . The interatomic forces in the simulations are represented by a classical many-body potential fitted against a high quality ab initio Born–Oppenheimer PES for the  $H + H_2$  reaction.<sup>30</sup> These and all subsequent calculations employ standard tools.<sup>31–33</sup> Full computational details and additional results are given in the [Supporting Information](#); sample inputs to reproduce the simulations are also deposited on PLUMED-NEST, the public repository of the PLUMED consortium,<sup>34</sup> as plumID:19.080.

As shown in [Figure 2a](#),  $p(u)$  of the D–D bond is dependent on the temperature; the distribution is wider at high  $T$ , and it can be anticipated that the higher probability to observe large bond stretching will increase the reactivity of the molecule. Moreover, it must be noted that  $p(u)$  is a classical, canonical distribution, which matches neither the distribution found in an energy-conserving QCT trajectory nor that of an excited quantum oscillator. Rather, it represents the distribution of an ensemble of differently excited molecules, which *on average* have a vibrational temperature  $T_{\text{vib}}$ .

[Figure 2b](#) shows the bias potential  $V(u)$  parametrized by VES to enforce  $p^*(u)$  for  $T_{\text{vib}} = 1500$  K at  $T_{\text{bg}} = 300$  K. When applied during an NVT simulation fully thermostated at 300 K, this bias can reproduce  $p(u)$  obtained from a simulation explicitly thermostated at 1500 K, as shown in [Figure 2c](#). We also note here that distribution  $p^*(u)$  is similar to a well-tempered distribution defined by the bias factor  $\gamma = T_{\text{vib}}/T_{\text{bg}}$ , as long as entropic contributions can be ignored; these subtle differences are further discussed in the [Supporting Information](#).

The  $D + D_2$  reaction is found to have a symmetric FES, as expected, with a barrier  $\Delta^\ddagger F$  of about 11.5 kcal/mol at 300 K ([Figure 2d](#)). The reaction revolves around a central atom  $D_B$  that is exchanged between atoms  $D_A$  and  $D_C$ ; the reaction coordinate  $s$  is in that case the difference in distances  $s = r_{AB} - r_{BC}$ . When applying the previously optimized  $V(u)$  associated with  $p^*(u)$  for  $T_{\text{vib}} = 1500$  K as a static bias to excite all D–D bonds in the system, modeling a vibrationally adiabatic process, the apparent free energy barrier  $\Delta^\ddagger F^*$  is greatly reduced to 5.5 kcal/mol. A shallow additional free energy minimum halfway along the reaction path can also be observed, which is qualitatively in line with literature results and corresponds to a bound  $D_3$  state.<sup>35</sup> At higher vibrational temperatures, this minimum further deepens.

[Figure 2e](#) shows how  $\Delta^\ddagger F^*$  varies in function of  $T_{\text{vib}}$ . It can be seen that upon heating of the stretch mode, the barrier initially decreases quite strongly. Starting around  $T_{\text{vib}} = 2000$  K, however, further increase of the vibrational temperature does not have much additional impact, reaching a minimum barrier of about 3.3 kcal/mol. These findings give direct mechanistic insight. Although vibrational energy is a very efficient promoter of the reaction, some translational energy is still required; D–D bond stretch predominantly contributes to the reaction coordinate, but the role of translational energy in the  $D \cdots D_2$  approach is still significant, as also reported in the literature.<sup>22</sup>

Chemical observables can also be directly computed from the apparent FES. As discussed in the [Supporting Information](#), we can use a slightly modified Eyring equation to compute reaction rate coefficients  $k$  as a function of  $T_{\text{vib}}$ , plotted in [Figure 2e](#).

Because of the MD time scale problem it is usually not possible to explicitly verify the assumptions in our model, which should normally be done by comparing these implicitly computed rate coefficients to those obtained from brute-force explicit MD simulations on the same PES. Fortunately, however, the PES for the hydrogen atom exchange reaction is very cheap to evaluate. Therefore, it is in this case possible to observe reactive events even during long (up to 200 ns) unbiased simulations, for  $T_{\text{vib}} \geq 1000$  K. In these simulations, vibrational nonequilibrium is achieved with a hot spot thermostat<sup>26</sup> which, unlike our proposed method, models vibrational excitation directly in phase space (i.e., including its kinetic component). As can be seen in [Figure 2e](#), these brute forced explicit rate coefficients agree very well with those computed through our own implicit approach, which achieves kinetic accuracy at a much lower cost. Thus, our purely configuration space-based biasing approach can even capture the kinetic effects arising from vibrational excitation.

Note that an explicit treatment of vibrational excitation with the hot spot thermostat cannot be carried out in conjunction with a bias-based free energy method. The thermostat selectively excites specific modes in the system based on their frequency; for  $D_2$ , we excite the region around  $3000 \text{ cm}^{-1}$ . However, the addition of a fluctuating bias potential throughout the simulation will modify the mode frequencies of interest in unpredictable ways, which would also change the effective  $T_{\text{vib}}$ .

Our approach can also be used to predict mode selectivities. As a paradigmatic example we take the symmetric  $S_N2$  reaction of deuterated methyl chloride,  $Cl^- + CD_3Cl$ . For this type of reaction, the stretch vibration of the carbon–halogen bond is known to stimulate the process, whereas the C–H stretch is a spectator.<sup>36</sup> These conclusions are also obtained using our method on the semiempirical PM6 PES<sup>37</sup> at  $T_{\text{bg}} = 300$  K, as shown in [Figure 3a](#). Excitation of the C–Cl stretch is not quite as efficient as the D–D stretch of the previous example (here, only about 50% of the excess vibrational energy is used to lower the barrier) but nevertheless stands in stark contrast with the C–D stretch. Indeed, with the C–Cl stretch at  $T_{\text{vib}} = 3000$  K we find a barrier reduced by almost 4 kcal/mol—from 8.60 to 4.64 kcal/mol—resulting in a rate enhancement of 3 orders of magnitude; in turn, a C–D stretch at the same  $T_{\text{vib}}$  has no appreciable effect on  $\Delta^\ddagger F^*$  at all. We note that we do not distinguish between the different symmetric and asymmetric C–D vibrations. For details, please see the [Supporting Information](#).

Other than confirming the known mode selectivity in well-studied reactions, our method can also predict vibrational efficacies in processes that are not yet characterized. As one such example, we take the addition reaction of a hydroxyl radical to  $CO_2$ , forming a bicarbonate radical  $HCO_3$  ([Figure 3b](#), inset), modeled by a self-consistent charge density functional tight-binding (SCC-DFTB) PES,<sup>38</sup> again at  $T_{\text{bg}} = 300$  K. The  $CO_2$  molecule has three distinct vibrational modes: a doubly degenerate bend, a symmetric stretch, and an asymmetric stretch. Interestingly, none of these vibrations involve bonds that are formed or broken during the reaction, making it difficult to intuitively assert which of these (if any)



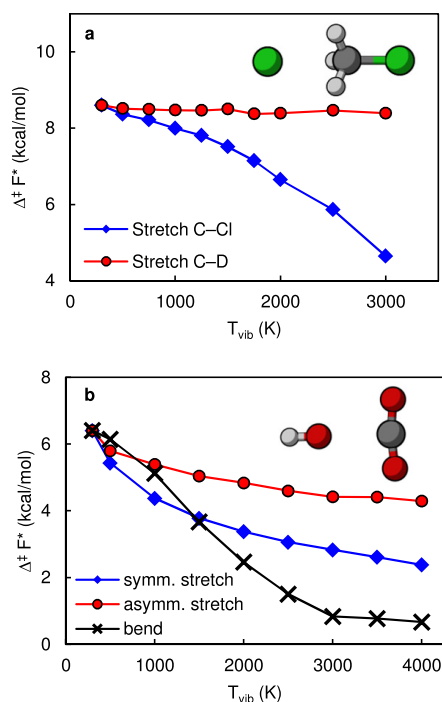


**Figure 3.** Predicting mode selectivity in terms of the apparent free energy barrier  $\Delta^\ddagger F^*$ . (a) C–Cl stretch versus C–D stretch in a symmetric nucleophilic substitution reaction. (b) Relative efficacy of different excited vibrational modes in  $\text{CO}_2$  for stimulating OH addition.

can stimulate the considered reaction—as opposed to the previous  $\text{S}_{\text{N}}2$  example. Our method provides answers. As shown in Figure 3b, the different mode-selective excitations have varying efficacies: excitation of the (combined) bending mode(s) has the strongest effect, reducing  $\Delta^\ddagger F^*$  to almost zero at  $T_{\text{vib}} = 4000$  K, while the two stretch modes are less efficient.

We can give these different efficacies an a posteriori rationalization. Although the bending mode does not directly involve the  $\text{OH}\cdots\text{CO}_2$  contact, the addition reaction requires a strong deformation of the O–C–O angle from  $180^\circ$  to about  $116^\circ$  which, judging by its role in vibrational reaction stimulation, appears to make a major contribution to the reaction coordinate. Similarly, both C–O bonds are somewhat stretched upon addition (from 1.16 to 1.28 Å), a motion that most closely resembles the symmetric stretch in  $\text{CO}_2$ , which might explain that mode's advantage over the asymmetric stretch. These observations underline our method's ability to unravel mechanistic details of reactions in a manner that complements chemical intuition and state-resolved experiments or simulations.

State-of-the-art free energy methods can produce accurate free energy surfaces or differences within fairly short (<1 ns) time scales. Therefore, our indirect approach to vibrationally stimulated reactions can be paired with both classical or ab initio force fields and, in principle, applied to arbitrary gas–gas or gas–surface reactions. This makes our method complementary to QCT simulations and considerably widens the scope of atomistic simulations of vibrationally stimulated reactions.

A possible application of our method is to study the effect of thermal nonequilibrium in plasma catalysis on the gas–surface chemistry, in order to compare its effects on the same footing as those of electronic nonequilibrium, i.e., plasma surface

charging;<sup>39,40</sup> surface reactions will also pose a more stringent test case with respect to the method's computational cost. Moreover, the precise relation between continuous energy distributions (as in our method) and state-resolved simulations (as in QCT) should be studied in order to correctly interpret the physical significance of using a classical energy spectrum.

Finally, we wish to draw attention to a related novel class of techniques: Within the framework of enhanced sampling methods, several approaches have been developed that can compute the contribution of different molecular degrees of freedom to the reaction dynamics.<sup>41–43</sup> These methods can be viewed as extensions of SVP that explicitly include the dynamical nature of the reaction and provide a more detailed decomposition of the reaction coordinate at a somewhat lower cost than our method, but they do not directly invoke the impact of vibrational nonequilibrium.

In conclusion, we have developed an indirect approach to study the effect of vibrational excitation on chemical reactions. The method can be applied to any reaction that can be studied with standard enhanced sampling techniques and yields the vibrational efficacy, mode selectivity, and reaction rate. Therefore, we expect that this approach will provide useful new insights into the reaction mechanisms of vibrationally excited molecules in technologies ranging from catalysis to plasma-based chemical conversion.

## ■ ASSOCIATED CONTENT

### Supporting Information

The Supporting Information is available free of charge at <https://pubs.acs.org/doi/10.1021/acs.jpcllett.9b03356>.

Full computational details, a note on the well-tempered ensemble, comments on the computation of reaction rate coefficients, plots of all  $p^*(u)$  and  $F^*(s)$  not in the main text, and numerical values of all barriers and rate coefficients reported in the graphs (PDF)

Sample input files to reproduce the simulations (ZIP)

## ■ AUTHOR INFORMATION

### Corresponding Author

\*E-mail: [kristof.bal@uantwerpen.be](mailto:kristof.bal@uantwerpen.be).

### ORCID

Kristof M. Bal: 0000-0003-2467-1223

Annemie Bogaerts: 0000-0001-9875-6460

Erik C. Neyts: 0000-0002-3360-3196

### Notes

The authors declare no competing financial interest.

## ■ ACKNOWLEDGMENTS

K.M.B. was funded as a junior postdoctoral fellow of the FWO (Research Foundation – Flanders), Grant 12ZI420N, and through a TOP-BOF research project of the University of Antwerp. The computational resources and services used in this work were provided by the VSC (Flemish Supercomputer Center), funded by the FWO and the Flemish Government—department EWI.

## ■ REFERENCES

- (1) Crim, F. F. Vibrational State Control of Bimolecular Reactions: Discovering and Directing the Chemistry. *Acc. Chem. Res.* **1999**, *32*, 877–884.

- (2) Wang, Y.; Song, H.; Szabó, I.; Czakó, G.; Guo, H.; Yang, M. Mode-Specific  $S_N2$  Reaction Dynamics. *J. Phys. Chem. Lett.* **2016**, *7*, 3322–3327.
- (3) Liu, K. Vibrational Control of Bimolecular Reactions with Methane by Mode, Bond, and Stereo Selectivity. *Annu. Rev. Phys. Chem.* **2016**, *67*, 91–111.
- (4) Beck, R. D.; Maroni, P.; Papageorgopoulos, D. C.; Dang, T. T.; Schmid, M. P.; Rizzo, T. R. Vibrational Mode-Specific Reaction of Methane on a Nickel Surface. *Science* **2003**, *302*, 98–100.
- (5) Juurlink, L. B. F.; Smith, R. R.; Killelea, D. R.; Utz, A. L. Comparative Study of C–H Stretch and Bend Vibrations in Methane Activation on Ni(100) and Ni(111). *Phys. Rev. Lett.* **2005**, *94*, 208303.
- (6) Killelea, D. R.; Campbell, V. L.; Shuman, N. S.; Utz, A. L. Bond-Selective Control of a Heterogeneously Catalyzed Reaction. *Science* **2008**, *319*, 790–793.
- (7) Crim, F. F. Chemical Dynamics of Vibrationally Excited Molecules: Controlling Reactions in Gases and on Surfaces. *Proc. Natl. Acad. Sci. U. S. A.* **2008**, *105*, 12654–12661.
- (8) Chen, J.; Zhou, X.; Zhang, Y.; Jiang, B. Vibrational Control of Selective Bond Cleavage in Dissociative Chemisorption of Methanol on Cu(111). *Nat. Commun.* **2018**, *9*, 4039.
- (9) Smith, R. R.; Killelea, D. R.; DelSesto, D. F.; Utz, A. L. Preference for Vibrational over Translational Energy in a Gas-Surface Reaction. *Science* **2004**, *304*, 992–995.
- (10) Fridman, A. *Plasma Chemistry*, 3rd ed.; Cambridge University Press: New York, 2008.
- (11) van Rooij, G. J.; van den Bekerom, D. C. M.; den Harder, N.; Minea, T.; Berden, G.; Bongers, W. A.; Engeln, R.; Graswinckel, M. F.; Zoethout, E.; van de Sanden, M. C. M. Taming Microwave Plasma to Beat Thermodynamics in CO<sub>2</sub> Dissociation. *Faraday Discuss.* **2015**, *183*, 233–248.
- (12) Neyts, E. C.; Ostrikov, K. K.; Sunkara, M. K.; Bogaerts, A. Plasma Catalysis: Synergistic Effects at the Nanoscale. *Chem. Rev.* **2015**, *115*, 13408–13446.
- (13) Mehta, P.; Barboun, P.; Herrera, F. A.; Kim, J.; Rumbach, P.; Go, D. B.; Hicks, J. C.; Schneider, W. F. Overcoming Ammonia Synthesis Scaling Relations with Plasma-Enabled Catalysis. *Nat. Catal.* **2018**, *1*, 269–275.
- (14) Nozaki, T.; Okazaki, K. Non-Thermal Plasma Catalysis of Methane: Principles, Energy Efficiency, and Applications. *Catal. Today* **2013**, *211*, 29–38.
- (15) Kim, J.; Abbott, M. S.; Go, D. B.; Hicks, J. C. Enhancing C–H Bond Activation of Methane via Temperature-Controlled, Catalyst–Plasma Interactions. *ACS Energy Lett.* **2016**, *1*, 94–99.
- (16) Sheng, Z.; Kameshima, S.; Yao, S.; Nozaki, T. Oxidation Behavior of Ni/Al<sub>2</sub>O<sub>3</sub> Catalyst in Nonthermal Plasma-Enabled Catalysis. *J. Phys. D: Appl. Phys.* **2018**, *51*, 445205.
- (17) Pratihari, S.; Ma, X.; Homayoon, Z.; Barnes, G. L.; Hase, W. L. Direct Chemical Dynamics Simulations. *J. Am. Chem. Soc.* **2017**, *139*, 3570–3590.
- (18) Zhou, X.; Nattino, F.; Zhang, Y.; Chen, J.; Kroes, G.-J.; Guo, H.; Jiang, B. Dissociative Chemisorption of Methane on Ni(111) Using a Chemically Accurate Fifteen Dimensional Potential Energy Surface. *Phys. Chem. Chem. Phys.* **2017**, *19*, 30540–30550.
- (19) Gerrits, N.; Shakouri, K.; Behler, J.; Kroes, G.-J. Accurate Probabilities for Highly Activated Reaction of Polyatomic Molecules on Surfaces Using a High-Dimensional Neural Network Potential: CHD<sub>3</sub> + Cu(111). *J. Phys. Chem. Lett.* **2019**, *10*, 1763–1768.
- (20) Kozák, T.; Bogaerts, A. Splitting of CO<sub>2</sub> by Vibrational Excitation in Non-Equilibrium Plasmas: A Reaction Kinetics Model. *Plasma Sources Sci. Technol.* **2014**, *23*, No. 045004.
- (21) Polanyi, J. C. Concepts in Reaction Dynamics. *Acc. Chem. Res.* **1972**, *5*, 161–168.
- (22) Jiang, B.; Guo, H. Relative Efficacy of Vibrational vs. Translational Excitation in Promoting Atom-Diatom Reactivity: Rigorous Examination of Polanyi's Rules and Proposition of Sudden Vector Projection (SVP) Model. *J. Chem. Phys.* **2013**, *138*, 234104.
- (23) Guo, H.; Jiang, B. The Sudden Vector Projection Model for Reactivity: Mode Specificity and Bond Selectivity Made Simple. *Acc. Chem. Res.* **2014**, *47*, 3679–3685.
- (24) Abrams, C.; Bussi, G. Enhanced Sampling in Molecular Dynamics Using Metadynamics, Replica-Exchange, and Temperature-Acceleration. *Entropy* **2014**, *16*, 163–199.
- (25) Valsson, O.; Parrinello, M. Variational Approach to Enhanced Sampling and Free Energy Calculations. *Phys. Rev. Lett.* **2014**, *113*, No. 090601.
- (26) Dettori, R.; Ceriotti, M.; Hunger, J.; Melis, C.; Colombo, L.; Donadio, D. Simulating Energy Relaxation in Pump–Probe Vibrational Spectroscopy of Hydrogen-Bonded Liquids. *J. Chem. Theory Comput.* **2017**, *13*, 1284–1292.
- (27) Ceriotti, M.; Bussi, G.; Parrinello, M. Langevin Equation with Colored Noise for Constant-Temperature Molecular Dynamics Simulations. *Phys. Rev. Lett.* **2009**, *102*, No. 020601.
- (28) Ceriotti, M.; Bussi, G.; Parrinello, M. Colored-Noise Thermostats à la Carte. *J. Chem. Theory Comput.* **2010**, *6*, 1170–1180.
- (29) Valsson, O.; Parrinello, M. Well-Tempered Variational Approach to Enhanced Sampling. *J. Chem. Theory Comput.* **2015**, *11*, 1996–2002.
- (30) Zhou, X. W.; Ward, D. K.; Foster, M.; Zimmerman, J. A. An Analytical Bond-Order Potential for the Copper–Hydrogen Binary System. *J. Mater. Sci.* **2015**, *50*, 2859–2875.
- (31) Plimpton, S. Fast Parallel Algorithms for Short-Range Molecular Dynamics. *J. Comput. Phys.* **1995**, *117*, 1–19.
- (32) Hutter, J.; Iannuzzi, M.; Schiffrmann, F.; VandeVondele, J. CP2K: Atomistic Simulations of Condensed Matter Systems. *WIREs Comput. Mol. Sci.* **2014**, *4*, 15–25.
- (33) Tribello, G. A.; Bonomi, M.; Branduardi, D.; Camilloni, C.; Bussi, G. PLUMED 2: New Feathers for an Old Bird. *Comput. Phys. Commun.* **2014**, *185*, 604–613.
- (34) The PLUMED consortium. Promoting Transparency and Reproducibility in Enhanced Molecular Simulations. *Nat. Methods* **2019**, *16*, 670–673.
- (35) Jankunas, J.; Sneha, M.; Zare, R. N.; Bouakline, F.; Althorpe, S. C.; Herráez-Aguilar, D.; Aoiz, F. J. Is the Simplest Chemical Reaction Really so Simple? *Proc. Natl. Acad. Sci. U. S. A.* **2014**, *111*, 15–20.
- (36) Stei, M.; Carrascosa, E.; Dörfler, A.; Meyer, J.; Olsz, B.; Czakó, G.; Li, A.; Guo, H.; Wester, R. Stretching Vibration is a Spectator in Nucleophilic Substitution. *Sci. Adv.* **2018**, *4*, eaas9544.
- (37) Stewart, J. J. P. Optimization of Parameters for Semiempirical Methods V: Modification of NDDO Approximations and Application to 70 Elements. *J. Mol. Model.* **2007**, *13*, 1173–1213.
- (38) Elstner, M.; Porezag, D.; Jungnickel, G.; Elsner, J.; Haugk, M.; Frauenheim, T.; Suhai, S.; Seifert, G. Self-Consistent-Charge Density-Functional Tight-Binding Method for Simulations of Complex Materials Properties. *Phys. Rev. B: Condens. Matter Mater. Phys.* **1998**, *58*, 7260–7268.
- (39) Bal, K. M.; Huygh, S.; Bogaerts, A.; Neyts, E. C. Effect of Plasma-Induced Surface Charging on Catalytic Processes: Application to CO<sub>2</sub> Activation. *Plasma Sources Sci. Technol.* **2018**, *27*, No. 024001.
- (40) Bal, K. M.; Neyts, E. C. Overcoming Old Scaling Relations and Establishing New Correlations in Catalytic Surface Chemistry: Combined Effect of Charging and Doping. *J. Phys. Chem. C* **2019**, *123*, 6141–6147.
- (41) Tiwary, P.; Berne, B. J. Spectral Gap Optimization of Order Parameters for Sampling Complex Molecular Systems. *Proc. Natl. Acad. Sci. U. S. A.* **2016**, *113*, 2839–2844.
- (42) McCarty, J.; Parrinello, M. A Variational Conformational Dynamics Approach to the Selection of Collective Variables in Metadynamics. *J. Chem. Phys.* **2017**, *147*, 204109.
- (43) Mendels, D.; Piccini, G.; Parrinello, M. Collective Variables from Local Fluctuations. *J. Phys. Chem. Lett.* **2018**, *9*, 2776–2781.